

# Demon driven by geometrical phase

Ryosuke Yoshii\*

Center for Liberal Arts and Sciences, Sanyo-Onoda City University, Yamaguchi 756-0884, Japan

Hisao Hayakawa†

Center for Gravitational Physics and Quantum Information,  
Yukawa Institute for Theoretical Physics, Kyoto University,  
Kitashirakawa-oiwake cho, Sakyo-ku, Kyoto 606-8502, Japan

(Dated: May 31, 2022)

We theoretically study an entropy production and a work extracted from a system connected to two reservoirs by periodic modulations of chemical potentials of the reservoirs and one parameter in the system Hamiltonian under an isothermal condition. We find that the modulation of parameters can drive a geometrical state, which is away from a nonequilibrium steady state. With the aid of this property, we construct a demon in which the relative entropy increases with time and we can extract the work, if we begin with the nonequilibrium steady state without modulations of parameters. We employ the Anderson model to demonstrate that the relative entropy can increase with time.

*Introduction.* - The second law of thermodynamics is one of the most fundamental laws in physics, which gives the upper bound of the available work that we can extract from reservoirs. Maxwell proposed an idealistic setup to violate the second law in which the demon quickly opens and closes the gate to allow only fast-moving molecules to pass through in one direction [1]. This leads to the decrement of the entropy without applying any work, and the violation of the second law of thermodynamics. Since Maxwell's original idea relies on the measurement of molecules, it is natural to combine the physical law and information science as information thermodynamics to realize Maxwell's demon [2–7].

Nevertheless, the cost of implementation of informational Maxwell's demon is expensive, though the theoretical formulation ignores its cost so far. Instead, we propose a geometrical demon with the aid of Berry's phase [8] in a geometrical engine as an extension of the Thouless pumping [9–11]. Let us consider a small system sandwiched between two reservoirs. If two parameters in the reservoirs and one parameter in a system Hamiltonian are controlled by an external agent, we can extract the work from the system. This is a natural application of the Thouless pumping [9–25] and geometrical thermodynamics [26–33]. It is known that the Kullback-Leibler (KL) is positive semidefinite, where its zero is only achieved if the system is in a nonequilibrium steady state (NESS) [31, 32, 34–39]. We note that the relative entropy can differ from the KL divergence. Indeed, the KL divergence is always zero for a completely periodic modulation, if we start from the NESS at which the KL divergence is zero because the KL divergence cannot increase for any completely positive and trace-preserving (CPTP) processes [34–39]. On the other hand, the relative entropy of the system during a cyclic modulation can

be positive and increase thanks to the existence of the geometrical phase. Thus, we may extract the work through this geometrical engine with the aid of the increment of the relative entropy.

*Geometrical phase and entropy production.*- In the present work, we focus on a system connected to two reservoirs. The left and right reservoirs are characterized by chemical potentials ( $\mu_L$  and  $\mu_R$ ) and a temperature  $T$ , respectively. We choose the control parameters to be chemical potentials in reservoirs and confining potential of the system under an isothermal condition.

We modulate the chemical potentials

$$\mu_L = \bar{\mu}(1 + r_L \sin \theta), \quad \mu_R = \bar{\mu}[1 + r_R \sin(\theta + \delta)], \quad (1)$$

where  $\bar{\mu} := \frac{1}{2\pi} \int_0^{2\pi} d\theta \mu_\alpha(\theta)$  is the one-cycle average of the chemical potential  $\mu_\alpha$  in the reservoir  $\alpha$  ( $=L$  or  $R$ ). We assume that  $\mu_\alpha$  only depends on the modulation phase  $\theta$ . We also assume that the system Hamiltonian  $\hat{H}(\lambda(\theta))$  is perfectly periodic, i. e.  $\hat{H}(\lambda(\theta)) = \hat{H}(\lambda(\theta + 2\pi))$  through a parameter  $\lambda(\theta)$  as  $\lambda(\theta) := 1 + r_H \cos \theta$ . To reduce the number of parameters we only consider the case of  $r := r_L = r_R = r_H$ . To keep the positivity of the parameters we assume  $|r| < 1$ . Thus, our system is characterized by a set of fixed parameters such as  $T$  and  $\bar{\mu}$ , and two control parameters  $r$  and  $\delta$ . To express the control parameters we introduce  $\mathbf{\Lambda} := (\lambda(\theta), \mu_L(\theta)/\bar{\mu}, \mu_R(\theta)/\bar{\mu})$  with using  $\Lambda_\mu$  for one of its components.

We consider the master equation for the density matrix  $\hat{\rho}(\theta)$ :

$$\frac{d}{d\theta} |\hat{\rho}(\theta)\rangle = \epsilon^{-1} \hat{K} |\hat{\rho}(\theta)\rangle, \quad (2)$$

where  $\hat{K}$  is the evolution operator. We have used the vector notation  $|\hat{\rho}(\theta)\rangle$  in Eq. (2), in which the components of the density matrix  $\hat{\rho}(\theta)$  align. Here, we use the scaled time  $\theta := \omega t$ , where  $\omega$  is the modulation angular frequency. We also introduce the dimensionless parameter  $\epsilon$  in Eq. (2) as  $\epsilon := 2\pi\omega/\Gamma$  where  $\Gamma$  is the bandwidth to characterize the hopping rate of electrons from

\* e-mail addressryoshii@rs.socu.ac.jp

† hisao@yukawa.kyoto-u.ac.jp

the reservoirs to the system. Introducing the eigenvalue  $\varepsilon_i$  by subscription  $i$  for  $\hat{K}$ , the corresponding left and right eigenstates  $\langle \ell_i |$  and  $| r_i \rangle$  satisfy the orthonormal relation  $\langle \ell_i | r_j \rangle = \delta_{ij}$ , if the eigenvalues are non-degenerate. We assume that there exists the non-degenerate largest eigenvalue  $\varepsilon_0 := 0$  corresponding to a steady-state. The probability conservation leads to the left zero eigenvector  $\langle \ell_0 |$  defined as  $\langle \ell_0 | \hat{K} = 0$  whose diagonal components in the matrix form are 1 and 0 otherwise. The right zero eigenstate  $| r_0 \rangle$  satisfying  $\hat{K} | r_0 \rangle = 0$  is also expressed as  $|\hat{\rho}^{\text{SS}}\rangle$  to specify the NESS.

Since all eigenvalues except for  $\varepsilon_0 = 0$  are negative, the physical state is relaxed to  $|\hat{\rho}^{\text{SS}}\rangle$  in the absence of the modulations. This suggests that the natural choice of the initial state would be  $|\hat{\rho}^{\text{SS}}\rangle$ . We note that the stability of the steady-state has been discussed in Ref. [32].

The entropy production during one-cycle modulation starting from  $\theta$  is given by

$$\Delta S(\theta) := S^{\text{HS}}(\hat{\rho}(2\theta) || \hat{\rho}^{\text{SS}}(\theta)) - S^{\text{HS}}(\hat{\rho}(2\pi + \theta) || \hat{\rho}^{\text{SS}}(2\pi + \theta)), \quad (3)$$

where we have introduced the Hatano-Sasa type relative entropy [40]:

$$S^{\text{HS}}(\hat{\rho} || \hat{\sigma}) := \text{Tr} [\hat{\rho} (\ln \hat{\rho} - \ln \hat{\sigma})]. \quad (4)$$

$\Delta S(\theta)$  in Eq. (3) is expected to be  $\Delta S(\theta) \geq 0$ , since the entropy increases with time as  $-\dot{S}^{\text{HS}} \geq 0$ , where  $\dot{S}^{\text{HS}} := (d/d\theta)S^{\text{HS}}$ . Nevertheless, if we begin with the initial condition  $\hat{\rho}(0) = \hat{\rho}^{\text{SS}}(0)$ , Eq. (3) leads to

$$\Delta S = -S^{\text{HS}}(\hat{\rho}(2\pi) || \hat{\rho}^{\text{SS}}(2\pi)) \leq 0, \quad (5)$$

where and hereafter we use  $\Delta S := \Delta S(0)$ , because  $S^{\text{HS}}$  is positive semidefinite. Note that  $S^{\text{HS}}$  decreases towards zero in the absence of the modulation [34–39]. The condition of  $\Delta S \geq 0$  is compatible with Eq. (5) only if  $\hat{\rho}(\theta)$  is always equal to  $\hat{\rho}^{\text{SS}}(\theta)$  for arbitrary  $\theta$ . In other words, if the density matrix can differ from  $\hat{\rho}^{\text{SS}}(\theta)$  at some  $\theta$ ,  $\Delta S$  is negative. Note that the decrement of the entropy can be easily observed in physical situations if we begin with the equilibrium (maximum entropy) state [41].

Let us assume that the initial state is steady state  $|\hat{\rho}(0)\rangle = |r_0\rangle = |\hat{\rho}^{\text{SS}}\rangle$ . As shown in Refs. [25, 42], we obtain:

$$|\hat{\rho}(\theta)\rangle \simeq |\hat{\rho}^{\text{SS}}(\theta)\rangle + \sum_{i \neq 0}^n C_i(\theta) |r_i(\theta)\rangle, \quad (6)$$

where

$$C_i(\theta) = - \int_0^\theta d\phi e^{\varepsilon_i^{-1} \int_\phi^\theta dz \varepsilon_i(z)} \langle \ell_i(\phi) | \frac{d}{d\phi} | r_0(\phi) \rangle. \quad (7)$$

We note that the trace preserving is always satisfied for arbitrary  $\theta$  from  $\langle \ell_0 | r_i \rangle = \delta_{0i}$ .

The expressions in Eqs. (6) and (7) are compatible with the slow modulation approximation employed in Ref. [32].

The leading contribution of the modulation on the entropy production appears from the second term on the right-hand side (RHS) of Eq. (6).

Equation (6) is an important relation, because  $\hat{\rho}(\theta)$  is deviated from  $\hat{\rho}^{\text{SS}}(\theta)$  if  $C_i \neq 0$ . Therefore, if  $C_i$  for some  $i$  is non-zero, the relative entropy  $S^{\text{HS}}$  is positive. Namely,  $S^{\text{HS}}$  can increase if the geometrical phase exists. Thus, our system can extract the work automatically from the reservoirs. This is the essence of the geometrical demon. Note that the density matrix is reduced to Eqs. (6) and (7) for  $\theta \gg 1$  regardless the initial condition as shown in Ref. [42], though the geometrical term becomes negligibly small for large  $\theta$ .

The second term on RHS of Eq. (6) is the Berry-Sinitsyn-Nemenman (BSN) connection. For a cyclic modulation satisfying  $|r_i(2\pi)\rangle = |r_i(0)\rangle$  the deviation from the initial state after one cycle modulation becomes

$$\Delta |\hat{\rho}\rangle := |\hat{\rho}(2\pi)\rangle - |\hat{\rho}(0)\rangle = \sum_{i \neq 0} C_i |r_i(0)\rangle \quad (8)$$

where

$$C_i := \int_0^{2\pi} d\phi e^{\varepsilon_i^{-1} \int_\phi^{2\pi} dz \varepsilon_i(z)} \mathcal{A}_i^\mu \frac{\partial \Lambda_\mu}{\partial \phi}. \quad (9)$$

Here we have introduced the BSN connection  $\mathcal{A}_i^\mu$  as

$$\mathcal{A}_i^\mu := -\langle \ell_i(\Lambda(\phi)) | \frac{\partial}{\partial \Lambda_\mu} | r_0(\Lambda(\phi)) \rangle. \quad (10)$$

According to  $\mathcal{A}_i^\mu$  we define the BSN curvature as

$$F_i^{\mu\nu}(\theta) := \left( \frac{\partial \mathcal{A}_i^\nu}{\partial \Lambda_\mu} \right)_\theta - \left( \frac{\partial \mathcal{A}_i^\mu}{\partial \Lambda_\nu} \right)_\theta. \quad (11)$$

Because of the damping factor in Eq. (9), the contribution of the BSN curvature is localized in time. If the BSN curvature is zero inside the trajectory, we find that  $\Delta S = 0$ , whereas it can be nonzero if the BSN curvature exists. These results can be used if we begin with the general initial condition as shown in Ref. [42].

Now, we discuss thermodynamic relations to construct the geometrical demon. Let us introduce the work  $W$  as [43, 44]

$$W := \int_0^{2\pi} d\theta \mathcal{P}(\theta), \quad (12)$$

where

$$\mathcal{P}(\theta) := \text{Tr} \left[ \hat{\rho}(\theta) \frac{\partial \hat{H}(\lambda(\theta))}{\partial \lambda(\theta)} \right] \dot{\lambda}(\theta). \quad (13)$$

The work  $W$  and power  $\mathcal{P}(\theta)$  can be positive or negative depending on the situation. The positive  $\mathcal{P}(\theta)$  is interpreted as the power supply by the external agent, while the negative  $\mathcal{P}(\theta)$  can be regarded as the power loss. One can introduce

$$\mathcal{P}_{A/R}(\theta) := \frac{\mathcal{P}(\theta) \pm |\mathcal{P}(\theta)|}{2}, \quad (14)$$

which satisfies  $\mathcal{P}_A(\theta) = \mathcal{P}(\theta)$  ( $\mathcal{P}_R(\theta) = -\mathcal{P}(\theta)$ ) if  $\mathcal{P}(\theta) > 0$  ( $\mathcal{P}(\theta) < 0$ ),  $\mathcal{P}_A(\theta) = 0$  ( $\mathcal{P}_R(\theta) = 0$ ) otherwise. We also introduce  $Q_{A/R}$

$$Q_{A/R} := \int_0^{2\pi} d\theta \mathcal{P}_{A/R}(\theta). \quad (15)$$

This  $Q_A$  is interpreted as the absorbing heat of the system, whereas  $Q_R$  is the releasing heat of the system. By definition, there is a trivial relation  $Q_A \geq |W| \geq W$ . If the work  $W$  is negative, the system can be regarded as an engine in which the work done by the system is larger than the work done by the reservoirs. In this situation ( $W < 0$ ) we can define the efficiency  $\eta$  as

$$\eta := \frac{|W|}{Q_A}. \quad (16)$$

Thus, to construct a geometrical demon we need  $W < 0$  to utilize the negative entropy production  $\Delta S < 0$ . As long as we know, we cannot determine the sign of  $W$  in general. Thus, we demonstrate that  $W$  can be negative with the aid of the Anderson model.

*Application to the Anderson model.*- Let us apply the general framework to the Anderson model for a quantum dot (QD) in which a single dot is coupled to two electron reservoirs [45]. Thus, the total Hamiltonian  $\hat{H}^{\text{tot}}$  is written as

$$\hat{H}^{\text{tot}} := \hat{H} + \hat{H}^r + \hat{H}^{\text{int}}, \quad (17)$$

where  $\hat{H}$ , reservoir Hamiltonian  $\hat{H}^r$  and interaction Hamiltonian  $\hat{H}^{\text{int}}$  are, respectively, given by

$$\hat{H} = \sum_{\sigma} \epsilon_0 \hat{d}_{\sigma}^{\dagger} \hat{d}_{\sigma} + U(\theta) \hat{n}_{\uparrow} \hat{n}_{\downarrow}, \quad (18)$$

$$\hat{H}^r = \sum_{\alpha, k, \sigma} \epsilon_k \hat{a}_{\alpha, k, \sigma}^{\dagger} \hat{a}_{\alpha, k, \sigma}, \quad (19)$$

$$\hat{H}^{\text{int}} = \sum_{\alpha, k, \sigma} V_{\alpha} \hat{d}_{\sigma}^{\dagger} \hat{a}_{\alpha, k, \sigma} + \text{h.c.}, \quad (20)$$

where  $\hat{a}_{\alpha, k, \sigma}^{\dagger}$  and  $\hat{a}_{\alpha, k, \sigma}$  are, respectively, the creation and annihilation operators for the electron in the reservoirs  $\alpha = (\text{L or R})$  with the wave number  $k$ , energy  $\epsilon_k$ , and spin  $\sigma = (\uparrow \text{ or } \downarrow)$ . Moreover,  $\hat{d}_{\sigma}^{\dagger}$  and  $\hat{d}_{\sigma}$  are those in the QD, respectively, and  $\hat{n}_{\sigma} = \hat{d}_{\sigma}^{\dagger} \hat{d}_{\sigma}$ .  $U(\theta) := U_0 \lambda(\theta)$  and  $V_{\alpha}$  are, respectively, the time-dependent electron-electron interaction in the QD and the transfer energy between QD and the reservoir  $\alpha$ . We adopt a model in the wide-band limit for the reservoirs. We denote, in this paper, the line width  $\Gamma = \pi \varrho (V_L^2 + V_R^2)$  where  $\varrho$  is the density of states in the reservoirs.

The Anderson model for the QD has the four states: the double occupied, singly occupied with an up-spin, singly occupied with a down-spin, and empty states. Therefore, the density matrix is expressed as a  $4 \times 4$  matrix. As shown in Ref. [32], however,  $\hat{\rho}(\theta)$  of the Anderson model under the wide-band approximation is reduced to a

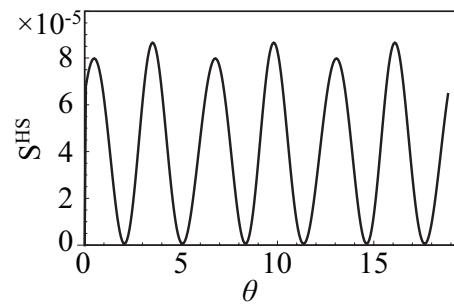


Figure 1. Time evolution of (a) relative entropy  $S^{\text{HS}}(\hat{\rho}(\theta) || \hat{\rho}^{\text{SS}}(\theta))$  for  $\delta = 0$ ,  $r = 0.9$  and  $\beta U_0 = 0.1$ .

diagonal matrix, where the diagonal elements correspond to the probability to find the states in the empty state  $\rho_e$ , the down-spin state  $\rho_{\downarrow}$ , the up-spin  $\rho_{\uparrow}$ , and the double occupied state  $\rho_d$ , respectively. The trace preserving condition  $\text{Tr} \hat{\rho} = \rho_e + \rho_{\uparrow} + \rho_{\downarrow} + \rho_d = 1$  reduces to the conservation of probability. This means that the model is a quasi-classical one. The explicit forms of the evolution matrix  $\hat{K}$  and the corresponding eigenstates  $\langle \ell_i |$  and  $| r_i \rangle$  are summarized in Ref. [42].

For the explicit calculation, we use Eqs. (6) and (7) with  $\theta = 2\pi$ . Integrating by part, one can show  $C_2(\theta) = 0$  since  $\langle \ell_2 |$  is independent of  $\theta$ .

One can verify  $\Delta S = 0$  for  $\beta \epsilon_0 \rightarrow \infty$  [42]. This implies that  $\hat{\rho}(\theta)$  has only the nonzero component  $\rho_e$  throughout the process. As a result, the entropy production by the geometrical phase is absent in this limit.

Hereafter, let us set  $\epsilon = 0.1$  and obtain some explicit results of the Anderson model. Recasting  $|\hat{\rho}(\theta)\rangle$  in matrix-form  $\hat{\rho}(\theta)$  and plugging it into Eq. (3), we obtain  $S^{\text{HS}}(\hat{\rho}(\theta) || \hat{\rho}^{\text{SS}}(\theta))$  and  $\Delta S$ . We plot the time evolution of  $S^{\text{HS}}(\hat{\rho}(\theta) || \hat{\rho}^{\text{SS}}(\theta))$  in Fig. 1 for  $\delta = 0$ ,  $r = 0.9$ , and  $\beta U_0 = 0.1$ . This figure clearly indicates the oscillation of  $S^{\text{HS}}(\hat{\rho}(\theta) || \hat{\rho}^{\text{SS}}(\theta))$  which increases at some instance. It is easy to verify that all components of  $\hat{\rho}(\theta)$  keep positivity during the dynamics [42], and thus, the dynamics keep the CPTP. Thus,  $S^{\text{HS}}(\hat{\rho}(\theta) || \hat{\rho}^{\text{SS}}(\theta))$  cannot be regarded as the KL-divergence. These results are obtained by the BSN connection  $C_i(\theta)$  in Eqs. (6) and (7), all of which are negative definite as shown in Ref. [42]. We also note that the behavior of  $S^{\text{HS}}(\theta)$  is almost periodic except for the quick relaxation process from the initial condition (see Fig. 1). This indicates that the dynamics are quickly reduced to the quasi-periodic state regardless of the initial condition, and thus,  $\Delta S(\theta)$  approaches zero in which the decay of  $\Delta S(\theta)$  can be approximated by an exponential function as can be seen in Fig. 2 [46].

Figure 3 (a) illustrates the contour of integral Eq. (9) in the parameter space  $(\mu_L(\theta), \mu_R(\theta), \theta)$ . As can be seen, the BSN curvature always exists, though the magnitude of them decreases with  $\theta$ . The BSN curvatures at specific  $\theta$ s are plotted in Figs. 3 (b) and (c), where the half-width of the peak or the dip are approximately located at  $\beta \bar{\mu} \approx 10$ .

Figure 4 is the plots of  $\Delta S$  versus  $\delta$  for various  $\beta U_0$  for

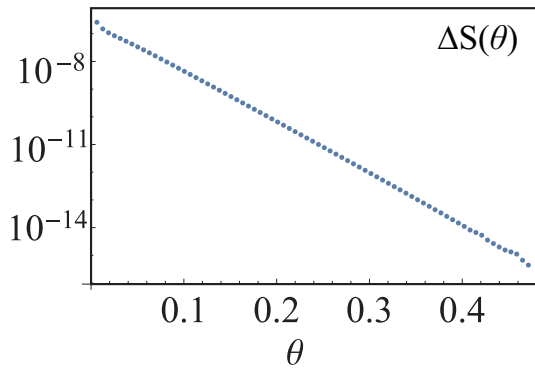


Figure 2. Plots of  $\Delta S(\theta)$  against  $\theta$  for  $\beta U_0 = 0.3$  and  $\delta = 0$  with  $r = 0.9$ .

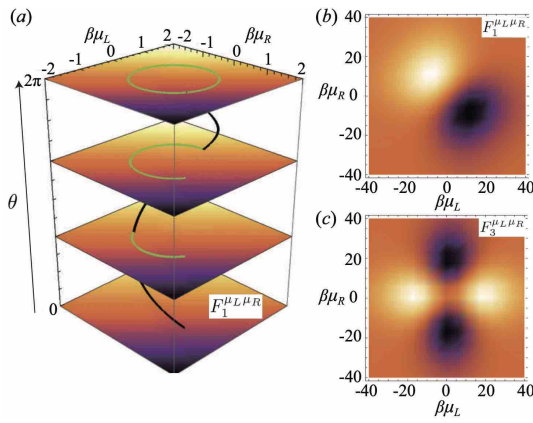


Figure 3. (a) Schematics of a contour of the integral of  $C_1$ , where the black solid line is the trajectory of the parameters. The color scale at a  $\theta$  expresses  $F_1^{\mu_L \mu_R}$ . (b) and (c) The BSN curvature  $F_1^{\mu_L \mu_R}$  and  $F_3^{\mu_L \mu_R}$  at  $\theta = 0$  are plotted. The parameters are set to be  $\beta \bar{\mu} = 0.1$ ,  $\beta U_0 = 0.1$  and  $\beta \epsilon_0 = 0.1$  for all figures.

$r = 0.9$ . In this range, the decrement  $\Delta S$  is enhanced as  $\beta U_0$  increases.

The work  $W$  defined in Eq. (12) also becomes negative as shown in Fig. 5 (a). This indicates that we can extract the work by the cyclic modulations of the parameters in the Anderson model without fine-tuning. In Fig. 5 (b) we plot the efficiency  $\eta$  defined in Eq. (16). These results are obtained from  $\Delta S < 0$  and, thus, our engine is suitable to call the geometrical demon.

*Concluding Remarks.*- We have implemented geometrical demon by the modulations of the chemical potentials in the reservoirs and the repulsion  $U$  in the system Hamiltonian under the isothermal condition. We can extract the work from this engine automatically with the increment of the relative entropy if we begin with the nonequilibrium steady state. Our geometrical demon does not need any observation of states to decrease the entropy. In this sense, our geometrical demon is easily implemented in realistic situations, and thus, we expect

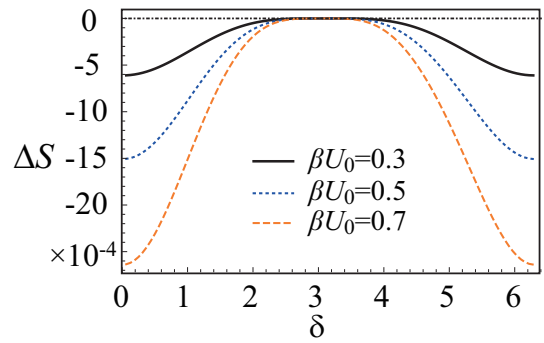


Figure 4. Plots of  $\Delta S$  against  $\delta$  for  $\beta U_0 = 0.3$  (solid line),  $0.5$  (dotted line),  $0.7$  (dashed line) with fixing  $r = 0.9$ .

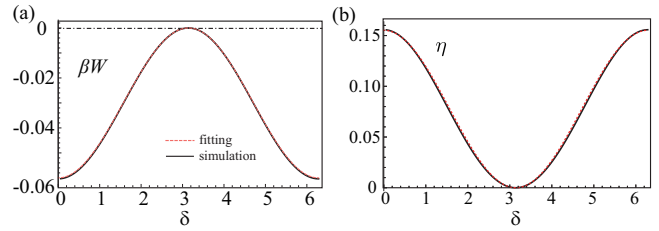


Figure 5. (a) Plots of the work done on the system in one-cycle modulation against  $\delta$  with  $\beta U_0 = 0.1$  and  $r = 0.9$  (solid line) and fitting by the sinusoidal function (dotted line). (b) Plots of the efficiency  $\eta$  for  $\beta U_0 = 0.1$  and  $r = 0.9$  (solid line) and fitting by the sinusoidal function (dotted line). The result of (a) and (b) are fitted by  $-0.3(\cos \delta + 1)$  and  $0.0766(\cos \delta + 1)$ , respectively.

wide applications of this demon, though it does not work after the second cycle. This means that we had better stop the modulation after one cycle and wait until the system reaches the NESS again, and restart the modulation to extract the work.

Our future tasks are as follows: (i) Because the present method for the argument is restricted to the case  $\epsilon \ll 1$ , we will need to extend the analysis to the regime of larger  $\epsilon$  as in Ref. [25]. (ii) Although we have analyzed a quantum system, our treatment is still quasi-classical. Thus, we have been unable to clarify the role of quantum coherence so far [30, 47, 48]. (iii) We have ignored the energy cost of controlling  $\lambda(\theta)$ ,  $\mu_L(\theta)$  and  $\mu_R(\theta)$ , but it is important when we consider the application of this geometrical demon. The estimation of the cost of controlling parameters is the most important task to be clarified, though the contribution of the house-keeping entropy in our system can be positive or negative depending on  $\delta$  [42].

*Acknowledgements.*- The authors thank Ville M. M. Paasonen, Kazutaka Takahashi, Kiyoshi Kanazawa, So-suke Ito, Hikaru Watanabe, and Asahi Yamaguchi for fruitful discussions and useful comments. This work is partially supported by a Grant-in-Aid of MEXT for Scientific Research KAKENHI (Grant Nos. 21H01006, 19K14616 and 20H01838).



- 
- [1] J. C. Maxwell, Theory of Heat (Appleton, London, 1871).
- [2] H. Touchette and S. Lloyd, Information-Theoretic Limits of Control. *Phys. Rev. Lett.* **84**, 1156 (2000).
- [3] T. Sagawa and M. Ueda, Generalized Jarzynski Equality under Nonequilibrium Feedback Control. *Phys. Rev. Lett.* **104**, 090602 (2010).
- [4] S. Viviana, C.-F. Lee, E. R. Key and D. A. Leigh, A molecular information ratchet, *Nature*. **445**, 523 (2007).
- [5] S. Toyabe, T. Sagawa, M. Ueda, E. Muneyuki and M. Sano, Experimental demonstration of information-to-energy conversion and validation of the generalized Jarzynski equality, *Nature Phys.* **6**, 988 (2010).
- [6] J. V. Koski, V. F. Maisi, T. Sagawa, and J. P. Pekola, Experimental Observation of the Role of Mutual Information in the Nonequilibrium Dynamics of a Maxwell Demon, *Phys. Rev. Lett.* **113**, 030601 (2014).
- [7] J. Parrondo, J. Horowitz and T. Sagawa, *Nature Phys.* **11**, 131 (2015).
- [8] M. V. Berry, Quantal phase factors accompanying adiabatic changes, *Proc. R. Soc. London Ser. A* **392**, 45 (1984).
- [9] D. J. Thouless, Quantization of particle transport, *Phys. Rev. B* **27**, 6083 (1983).
- [10] N. A. Sinitsyn and I. Nemenman, The Berry phase and the pump flux in stochastic chemical kinetics, *Europhys. Lett.* **77**, 58001 (2007).
- [11] N. A. Sinitsyn and I. Nemenman, Universal Geometric Theory of Mesoscopic Stochastic Pumps and Reversible Ratchets, *Phys. Rev. Lett.* **99**, 220408 (2007).
- [12] L. P. Kouwenhoven, A. T. Johnson, N. C. van der Vaart, C. J. P. M. Harmans, and C. T. Foxon, Quantized current in a quantum-dot turnstile using oscillating tunnel barriers, *Phys. Rev. Lett.* **67**, 1626 (1991).
- [13] H. Pothier, P. Lafarge, C. Urbina, D. Esteve, and M. H. Devoret, Single-Electron Pump Based on Charging Effects, *Europhys. Lett.* **17**, 249 (1992).
- [14] M. Switkes, C. M. Marcus, K. Campman, and A. C. Gossard, An Adiabatic Quantum Electron Pump, *Science* **283**, 1905 (1999).
- [15] A. Fuhrer, C. Fasth, and L. Samuelson, Single electron pumping in InAs nanowire double quantum dots, *Appl. Phys. Lett.* **91**, 052109 (2007).
- [16] S. K. Watson, R. M. Potok, C. M. Marcus, and V. Umansky, Experimental Realization of a Quantum Spin Pump, *Phys. Rev. Lett.* **91**, 258301 (2003).
- [17] P. W. Brouwer, Scattering approach to parametric pumping, *Phys. Rev. B* **58**, R10135 (1998).
- [18] J. Ren, P. Hänggi, and B. Li, Berry-Phase-Induced Heat Pumping and Its Impact on the Fluctuation Theorem, *Phys. Rev. Lett.* **104**, 170601 (2010).
- [19] T. Sagawa and H. Hayakawa, Geometrical expression of excess entropy production, *Phys. Rev. E* **84**, 051110 (2011).
- [20] T. Yuge, T. Sagawa, A. Sugita, and H. Hayakawa, Geometrical pumping in quantum transport: Quantum master equation approach, *Phys. Rev. B* **86**, 235308 (2012).
- [21] T. Yuge, T. Sagawa, A. Sugiura, and H. Hayakawa, Geometrical Excess Entropy Production in Nonequilibrium Quantum Systems, *J. Stat. Phys.* **153**, 412 (2013).
- [22] K. L. Watanabe and H. Hayakawa, Geometric fluctuation theorem for a spin-boson system, *Phys. Rev. E* **96**, 022118 (2017).
- [23] Y. Hino and H. Hayakawa, Fluctuation relations for adiabatic pumping, *Phys. Rev. E* **120**, 012115 (2020).
- [24] K. Takahashi, Y. Hino, K. Fujii and H. Hayakawa, Full Counting Statistics and Fluctuation? Dissipation Relation for Periodically Driven Two-State Systems, *J. Stat. Phys.* **181**, 2206 (2020).
- [25] K Takahashi, K Fujii, Y Hino, and H Hayakawa, Nonadiabatic Control of Geometric Pumping, *Phys. Rev. Lett.* **124**, 150602 (2020).
- [26] Z. Wang, L. Wang, J. Chen, C. Wang and J. Rie, Geometric heat pump: Controlling thermal transport with time-dependent modulations *Frontier, Phys.* **17**, 13201 (2022).
- [27] G. E. Crooks, Measuring Thermodynamic Length, *Phys. Rev. Lett.* **99**, 100602 (2007).
- [28] B. Bhandari, P. T. Alonso, F. Taddei, F. von Oppen, R. Fazio and L. Arrachea, Geometric properties of adiabatic quantum thermal machines, *Phys. Rev. B* **102**, 155407 (2020),
- [29] P Abiuso, H. J. D. Miller, M. Perarnau-Llobet, and M Scandi, Geometric optimisation of quantum thermodynamic processes, *Entropy* **22**, 1076 (2020).
- [30] K. Brandner and K. Saito, Thermodynamic Geometry of Microscopic Heat Engines, *Phys. Rev. Lett.* **124**, 040602 (2020).
- [31] Y. Hino and H. Hayakawa, Geometrical formulation of adiabatic pumping as a heat engine, *Phys. Rev. Research* **3**, 013187 (2021).
- [32] H. Hayakawa, V. M. M. Paasonen, and R. Yoshii, “Geometrical Quantum Chemical Engine”, arXiv:2112.12370 (2021).
- [33] J. Lu, Z. Wang, J. Peng, C. Wang, J.-H. Jiang and J. Ren, Geometric thermodynamic uncertainty relation in a periodically driven thermoelectric heat engine *Phys. Rev. B.* **105**, 115428 (2022).
- [34] S. Kullback, and R. A. Leibler, On information and sufficiency, *Annal. Math. Stat.*, **22**, 79 (1951).
- [35] T. Sagawa, Entropy, Divergence, and Majorization in Classical and Quantum Thermodynamics, to be published in Springer-Brief in Mathematical Physics arXiv:2007.09974.
- [36] D. Petz, Quasi-entropies for finite quantum systems, *Rep. Math. Phys.* **23**, 57 (1986).
- [37] D. Petz, Monotonicity of quantum relative entropy revisited, *Rev. Math. Phys.* **15**, 79 (2003)
- [38] M. B. Ruskai, Inequalities for quantum entropy: A review with conditions for equality, *J. Math. Phys.* **43**, 4358 (2002).
- [39] F. Hiai, M. Mosonyi, D. Petz, and C. Bény, Quantum f-divergences and error correction, *Rev. Math. Phys.* **23**, 691 (2011).
- [40] T. Hatano and S.-i. Sasa, Steady-State Thermodynamics of Langevin Systems, *Phys. Rev. Lett.* **86**, 3463 (2001).
- [41] As can be seen in the relation  $S^{\text{HS}}(\hat{\rho}^{\text{SS}}(\theta) || \hat{\rho}^{\text{SS}}(\theta)) = 0$ , our formulation has already eliminated the energy supply (from the connection with higher chemical potential) and dissipation (from the connection with the lower chemical potential) terms, which are perfectly balanced with each other in the nonequilibrium steady state. Thus, the Joule heat term does not appear explicitly in our formulation.
- [42] See Supplemental Material.
- [43] G. Benenti, G. Casati, K. Saito, and R. S. Whitney, *Phys.*

Rep. **694**, 1 (2017).

- [44] G. Kurizki and A. G. Kofman, *Thermodynamics and Control of Open Quantum Systems* (Cambridge Univ. Press, Cambridge, 2022).
- [45] Though there exist higher energy levels in realistic quantum dot systems, here we only consider the single energy level for simplicity.
- [46] Needless to say, the system with  $\Delta S < 0$  is not perfectly periodic even if  $\hat{H}(\lambda(\theta))$  and the control parameters are periodic. Since there exists a damping factor in the geometrical contribution,  $|\Delta S|$  in the second cycle is expected to be smaller than that in the first cycle. In the long time limit, the system asymptotically reaches the NESS in which the geometrical contribution asymptotically is negligible.
- [47] A. A. Svidzinsky, K. E. Dorfman, M. O. Scully, Enhancing photocell power by noise-induced coherence, *Coherent Opt. Phenomena*, **1**, 7 (2012).
- [48] J. Um, K. E. Dorfman and H. Park, Coherence enhanced quantum-dot heat engine, arXiv:2111.09582.

This Supplemental Material explains the details of calculations that are not involved in the main text. In Sec. I we derive a general expression of the time evolution of the density matrix  $\hat{\rho}(\theta)$  without a specific choice of the model and initial condition. In Sec. II we explain the contribution of the house-keeping entropy, which has been ignored in the main text. In Sec. III we present the detailed properties of the Anderson model. In Sec. IV we briefly summarize the differences between our analysis and the analysis in Ref. [S1].

## I. TIME EVOLUTION OF THE DENSITY MATRIX

This section consists of two subsections. In the first part IA, we derive the time evolution of  $\hat{\rho}(\theta)$  from the general initial condition to demonstrate the universality of Eqs. (6) and (7) for  $\theta \gg 1$ . In the second part IB, we present the detailed derivations of the BSN connection and BSN curvature.

### A. The derivation of the time-dependent expression of the density matrix starting from the general initial condition

The purpose of this section is to derive Eqs. (6) and (7). Although we assumed that the initial state is given by  $\hat{\rho}^{\text{SS}}(0)$ , we can derive these equations even we begin with the generalized initial condition

$$|\hat{\rho}_{\text{ini}}\rangle = \sum_i a_i |r_i(0)\rangle, \quad (\text{S1})$$

where  $a_i$  is given by

$$a_i := \langle \ell_i(0) | \hat{\rho}_{\text{ini}} \rangle. \quad (\text{S2})$$

We note that the normalization of the density matrix fixes the coefficient  $a_0$  to be 1 since

$$\text{Tr} \hat{\rho}_{\text{ini}} = \langle \ell_0 | \hat{\rho}_{\text{ini}} \rangle = \sum_i a_i \langle \ell_0 | r_i(0) \rangle = a_0 = 1. \quad (\text{S3})$$

One can derive  $|\hat{\rho}(\theta)\rangle$  for  $|\hat{\rho}(0)\rangle = |\hat{\rho}_{\text{ini}}\rangle$  as

$$\begin{aligned} & |\hat{\rho}(\theta + \Delta\theta)\rangle \\ & \simeq \sum_{i,j,k,\dots,l,m} a_m |r_i(\theta)\rangle e^{\varepsilon_i(\theta) \frac{\Delta\theta}{\varepsilon}} \langle \ell_i(\theta) | r_j(\theta - \Delta\theta)\rangle \\ & \quad \times e^{\varepsilon_j(\theta - \Delta\theta) \frac{\Delta\theta}{\varepsilon}} \langle \ell_j(\theta - \Delta\theta) | r_k(\theta - 2\Delta\theta)\rangle \\ & \quad \dots \times e^{\varepsilon_l(\Delta\theta)} \langle \ell_l(0) | r_m(0)\rangle \\ & = \sum_m a_m e^{\int_0^\theta \varepsilon_m(\phi) \frac{d\phi}{\varepsilon}} |r_m(\theta)\rangle + \sum_{m,n} C_{mn} a_n |r_m(\theta)\rangle, \quad (\text{S4}) \end{aligned}$$

where  $C_{mn}$  is given by

$$C_{mn}(\theta) = - \int_0^\theta d\phi e^{\int_\phi^\theta \varepsilon_m(\xi) \frac{d\xi}{\varepsilon}} e^{\int_0^\phi \varepsilon_n(\zeta) \frac{d\zeta}{\varepsilon}} \langle \ell_m(\phi) | \frac{d}{d\phi} | r_n(\phi) \rangle. \quad (\text{S5})$$

The phase factor in the first term on RHS of Eq. (S4) is the dynamical phase, while the second term on RHS is the term generated by the geometrical phase. Plugging  $\int_{\phi}^{\theta} \varepsilon_m(\xi) \frac{d\xi}{\epsilon} = \int_0^{\theta} \varepsilon_m(\xi) \frac{d\xi}{\epsilon} - \int_0^{\phi} \varepsilon_m(\xi) \frac{d\xi}{\epsilon}$  in Eq. (S5) and substituting it into Eq. (S4), we obtain

$$|\hat{\rho}(\theta)\rangle \simeq \sum_m a_m |\tilde{r}_m(\theta)\rangle + \sum_{m,n} \tilde{C}_{mn} a_n |\tilde{r}_m(\theta)\rangle, \quad (\text{S6})$$

where we have introduced

$$\tilde{C}_{mn}(\theta) := - \int_0^{\theta} d\phi \langle \tilde{\ell}_m(\phi) | \left( \frac{d}{d\phi} - \frac{\varepsilon_n}{\epsilon} \right) | \tilde{r}_n(\phi) \rangle, \quad (\text{S7})$$

$$|\tilde{r}_m(\theta)\rangle := e^{\epsilon^{-1} \int_0^{\theta} \varepsilon_m(\phi) d\phi} |r_m(\theta)\rangle, \quad (\text{S8})$$

and

$$\langle \tilde{\ell}_m(\theta) | := \langle \ell_m(\theta) | e^{-\epsilon^{-1} \int_0^{\theta} \varepsilon_m(\phi) d\phi}. \quad (\text{S9})$$

The orthonormal relation  $\langle \ell_m | r_n \rangle = \delta_{mn}$  leads to

$$\langle \tilde{\ell}_m(\theta) | \tilde{r}_n(\theta) \rangle = e^{-\int_0^{\theta} \varepsilon_m(\phi) \frac{d\phi}{\epsilon}} e^{\int_0^{\theta} \varepsilon_n(\phi) \frac{d\phi}{\epsilon}} \delta_{mn} = \delta_{mn}. \quad (\text{S10})$$

Substituting this into Eq. (S7) we obtain

$$\tilde{C}_{mn}(\theta) = \frac{\delta_{mn}}{\epsilon} \int_0^{\theta} d\phi \varepsilon_n(\phi) - \int_0^{\theta} d\phi \langle \tilde{\ell}_m(\phi) | \frac{d}{d\phi} | \tilde{r}_n(\phi) \rangle. \quad (\text{S11})$$

Equations (S6) and (S11) are the expressions of the time evolution starting from the general initial condition in Eq. (S1).

Note that the trace of  $\hat{\rho}(\theta)$  is always equal to the unity. It can be proved as follows. The coefficient  $C_{0j}$  identically vanishes since

$$\begin{aligned} \langle \tilde{\ell}_0(\phi) | \frac{\partial}{\partial \Lambda_\mu} | \tilde{r}_j(\phi) \rangle &= \frac{\partial \langle \tilde{\ell}_0(\phi) |}{\partial \Lambda_\mu} | \tilde{r}_j(\phi) \rangle - \frac{\partial}{\partial \Lambda_\mu} \langle \tilde{\ell}_0(\phi) | \tilde{r}_j(\phi) \rangle \\ &= 0. \end{aligned} \quad (\text{S12})$$

Thus,  $\text{Tr} \hat{\rho}(\theta)$  satisfies

$$\text{Tr} \hat{\rho}(\theta) = \langle \ell_0 | \hat{\rho}(\theta) \rangle = a_0 = 1, \quad (\text{S13})$$

where we have used  $\varepsilon_0(\phi) = 0$  and Eq. (S10).

Now, let us consider the behavior for  $\theta/\epsilon \gg 1$ . It is obvious that the first term on RHS of Eq. (S6) is reduced to  $|\hat{\rho}^{\text{SS}}(\theta)\rangle$  because the exponential damping factor for  $m \neq 0$  is negligible. Thus, Eq. (S6) is reduced to

$$|\hat{\rho}(\theta)\rangle \simeq |\hat{\rho}^{\text{SS}}(\theta)\rangle + \sum_{m,n} C_{mn}(\theta) a_n |r_m(\theta)\rangle \quad (\text{S14})$$

for  $\theta/\epsilon \gg 1$ . It is straightforward to evaluate  $C_{mn}(\theta)$  for  $n \neq 0$  as

$$\begin{aligned} |C_{mn}(\theta)| &= \left| \int_0^{\theta} d\phi e^{\int_{\phi}^{\theta} \varepsilon_m(\xi) \frac{d\xi}{\epsilon}} e^{\int_0^{\phi} \varepsilon_n(\xi) \frac{d\xi}{\epsilon}} \langle \ell_m(\phi) | \frac{d}{d\phi} | r_n(\phi) \rangle \right| \\ &\leq \int_0^{\theta} d\phi e^{\int_{\phi}^{\theta} \varepsilon_m(\xi) \frac{d\xi}{\epsilon}} e^{\int_0^{\phi} \varepsilon_n(\xi) \frac{d\xi}{\epsilon}} \left| \langle \ell_m(\phi) | \frac{d}{d\phi} | r_n(\phi) \rangle \right| \\ &\leq \int_0^{\theta} d\phi e^{\int_0^{\theta} \max(\varepsilon_m, \varepsilon_n)(\xi) \frac{d\xi}{\epsilon}} \left| \langle \ell_m(\phi) | \frac{d}{d\phi} | r_n(\phi) \rangle \right|. \end{aligned} \quad (\text{S15})$$

Thus,  $C_{mn}$  with  $n \neq 0$  is much smaller than  $C_{m0}$  because of the existence of the exponential factor in Eq. (S15).

Equation (S14) implies that the relative entropy  $\Delta S(\theta)$  approaches 0 in the absence of the geometrical phase whereas that is not achieved in the presence of the geometrical phase. Moreover, the relative entropy becomes non-zero as one can see from the result in the main text. Thus, the geometrical phase prevents the system from the relaxation towards the NESS at which the relative entropy  $S^{\text{HS}}$  is zero. Once we start to modulate the parameters, the system is driven from the NESS state. However, because of the exponential factor in Eq. (S5), which truncates the contribution in the integration except for  $\phi \approx \theta$ , the system again exhibits the periodic behavior in  $\theta$  after the characteristic time given by the eigenvalues of  $\hat{K}$ . As a result, the relative entropy  $S^{\text{HS}}$  also becomes periodic in  $\theta$  after some characteristic time  $\theta_c$ . Thus the relative entropy  $\Delta S(\theta)$  is expected to be zero for  $\theta > \theta_c$ . In Fig. 2, we plot the  $\theta$  dependence of  $\Delta S(\theta)$ . The figure clearly shows that  $\Delta S(\theta)$  exponentially approaches zero.

## B. Derivation of BSN connection and BSN curvature

For the cyclic modulation  $|r_i(2\pi)\rangle = |r_i(0)\rangle$ , the time evolution from the general initial state becomes

$$\begin{aligned} \Delta |\hat{\rho}\rangle &= \sum_{i \neq 0} a_i \left( e^{\int_0^{2\pi} \varepsilon_i(\phi) \frac{d\phi}{\epsilon}} - 1 \right) |r_i(0)\rangle \\ &\quad + \sum_{i,j} C_{ij} a_j e^{\int_0^{2\pi} \varepsilon_i(\phi) \frac{d\phi}{\epsilon}} |r_i(0)\rangle, \end{aligned} \quad (\text{S16})$$

where

$$C_{ij} := \delta_{ij} \oint_{\partial\Omega} d\phi \frac{\varepsilon_i(\phi)}{\epsilon} - \oint_{\partial\Omega} d\Lambda_\mu \mathcal{A}_{ij}^\mu \quad (\text{S17})$$

with the introduction of the BSN connection  $\mathcal{A}_{ij}^\mu$ :

$$\mathcal{A}_{ij}^\mu := \langle \tilde{\ell}_i(\phi) | \frac{\partial}{\partial \Lambda_\mu} | \tilde{r}_j(\phi) \rangle. \quad (\text{S18})$$

Here the summation in the first term on RHS of Eq. (S16) is taken except for  $i = 0$  since  $\varepsilon_0(\phi) = 0$  always gives  $e^{\int_0^{\theta} \varepsilon_0(\phi) d\phi} = 1$ . By using the Stokes theorem, we can rewrite Eq. (S17) as

$$C_{ij} = \delta_{ij} \oint_{\partial\Omega} d\phi \frac{\varepsilon_i(\phi)}{\epsilon} - \int_{\Omega} dS_{\mu\nu} F_{ij}^{\mu\nu}, \quad (\text{S19})$$

where  $\Omega$  is the area enclosed by the closed trajectory  $\partial\Omega$ ,  $S_{\mu\nu} = \frac{1}{2} d\Lambda_\mu \wedge d\Lambda_\nu$ , and  $F_{ij}^{\mu\nu}$  is the BSN curvatures defined as

$$F_{ij}^{\mu\nu} := \frac{\partial \langle \tilde{\ell}_i | \partial | \tilde{r}_j \rangle}{\partial \Lambda_\nu \partial \Lambda_\mu} - \frac{\partial \langle \tilde{\ell}_i | \partial | \tilde{r}_j \rangle}{\partial \Lambda_\mu \partial \Lambda_\nu}. \quad (\text{S20})$$

It is also possible to rewrite (S19) as

$$C_{ij} = \delta_{ij} \oint_{\partial\Omega} d\phi \frac{\varepsilon_i(\phi)}{\epsilon} + \frac{1}{2} \int_{\Omega} d\langle \tilde{\ell}_i | \wedge d | \tilde{r}_j \rangle. \quad (\text{S21})$$

## II. CONTRIBUTION OF THE HOUSE-KEEPING ENTROPY

The nonequilibrium system we consider is sustained by external agents, which needs the house-keeping heat as well as excess heat, though the main text only contains the description for the excess part [S2, S3]. In this section, we evaluate the house-keeping entropy production in our system.

As shown in Refs. [S2, S3], we usually introduce the counting field to calculate physical observables. As a result, Eq. (2) is formally modified as

$$\frac{d}{d\theta} |\hat{\rho}(\theta, \chi)\rangle = \epsilon^{-1} \hat{K}^\chi |\hat{\rho}(\theta, \chi)\rangle, \quad (\text{S22})$$

where  $\chi$  is the counting field, and  $|\hat{\rho}(\theta, \chi)\rangle$  and  $\hat{K}^\chi$  are the generalized density matrix and evolution operator, respectively. The generating function defined as

$$G_\theta(\chi) := \ln \text{Tr} \hat{\rho}(\theta, \chi) \quad (\text{S23})$$

plays an important role in this formulation, because we can evaluate the observable as  $\partial G_\theta(\chi)/\partial(i\chi)|_{\chi=0}$ . Since  $\hat{\rho}(\theta, \chi)$  behaves as  $\hat{\rho}(\chi) \sim \exp[\lambda_0(\mathbf{\Lambda}, \chi)\theta/\epsilon]$  for large  $\theta/\epsilon$  with the smallest eigenvalue  $\lambda_0(\mathbf{\Lambda}, \chi)$  of  $\hat{K}^\chi$  (which is reduced to zero in the limit  $\chi \rightarrow 0$ ) under a fixed  $\mathbf{\Lambda}$ , the house-keeping entropy flux [S2, S3] exists as

$$J_{\text{hk}}(\phi) := \left. \frac{\partial \lambda_0(\mathbf{\Lambda}(\phi), \chi)}{\partial(i\chi)} \right|_{\chi=0}. \quad (\text{S24})$$

This house-keeping entropy flux is dominant to maintain the steady-state.

Thus, time-averaged house-keeping entropy production during one cycle is given by

$$\overline{S}_{\text{hk}}(\theta) := \int_\theta^{\theta+2\pi} d\phi J_{\text{hk}}(\phi). \quad (\text{S25})$$

More explicitly,  $\hat{K}^\chi$  in Eq. (S22) can be written as

$$\hat{K}^\chi = \hat{K} + i\chi \hat{\mathcal{K}} + O(\chi^2), \quad (\text{S26})$$

the statement that  $\overline{S}_{\text{hk}}$  is zero. For explicit calculation of Eq. (S25) we employ the Anderson model as in the main text. In this case, as shown in Ref. [S4],  $\lambda_0(\mathbf{\Lambda}, \chi)$ ,  $\hat{\mathcal{K}}$  in Eq. (S26) is given by

$$\mathcal{K} := \begin{pmatrix} 0 & g_1 & g_1 & 0 \\ g_1 - 1 & 0 & 0 & g_0 \\ g_1 - 1 & 0 & 0 & g_0 \\ 0 & g_0 - 1 & g_0 - 1 & 0 \end{pmatrix} \quad (\text{S27})$$

with  $g_0 := (1 + e^{-\beta(\epsilon_0 - \mu_L)})^{-1}$  and  $g_1 := (1 + e^{-\beta(\epsilon_0 + U_0 - \mu_L)})^{-1}$ . Thus, we obtain  $\lambda_0(\mathbf{\Lambda}(\phi), \chi) = 0 + i\chi \lambda_0^{(1)}(\mathbf{\Lambda}(\phi)) + O(\chi^2)$  with

$$\lambda_0^{(1)}(\mathbf{\Lambda}(\phi)) = \langle \ell_0 | \mathcal{K}(\mathbf{\Lambda}(\phi)) | r_0 \rangle. \quad (\text{S28})$$

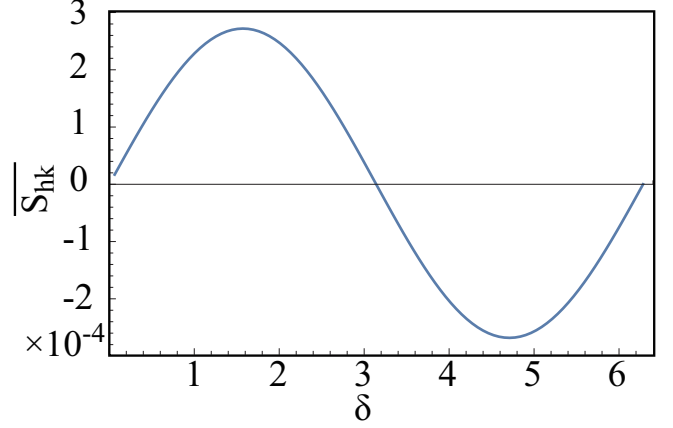


Figure S6. The time-averaged house-keeping entropy production during one cycle as a function of  $\delta$ . Here we set  $r = 0.9$  and  $\beta U_0 = 0.1$ .

As a result, the time-averaged house-keeping entropy production during one cycle S25 becomes

$$\overline{S}_{\text{hk}}(\theta) = \int_\theta^{2\pi+\theta} d\phi \langle \ell_0 | \mathcal{K}(\mathbf{\Lambda}(\phi)) | r_0 \rangle. \quad (\text{S29})$$

We note that  $\overline{S}_{\text{hk}}(\theta)$  is independent of  $\theta$ , because  $\lambda_0(\mathbf{\Lambda}(\phi), \chi)$  depends on  $\phi$  only through the periodic function  $\mathbf{\Lambda}(\phi)$ . In Fig. S6, we plot the house-keeping entropy production S29 in the case of the Anderson model. As shown in the figure, the house-keeping entropy production during one cycle can be positive or negative. It reflects the current-like behavior of the house-keeping entropy. In the cases of completely symmetric  $\delta = 0$  (no current flow) and completely asymmetric  $\delta = \pi$  (perfect compensation), the house-keeping entropies become zero.

## III. PROPERTIES OF THE ANDERSON MODEL

This section summarizes the detailed properties of the Anderson model. This section consists of four subsections. In the first subsection, we summarize the evolution matrix and eigenstates in the Anderson model. In the second subsection, we present the explicit form of the density matrix. In the third subsection, we write the explicit forms of BSN connection and BSN curvature as well as the expansion coefficients. In the last subsection, we present some detailed calculations for the Anderson model.

### A. Evolution matrix and eigenstates in the Anderson model

In this section, we summarize the evolution matrix and eigenstates in the Anderson model. Most of them can be found in Ref. [S32].



Since  $\hat{\rho}$  is a diagonal matrix,  $|\hat{\rho}\rangle$  has also only four component and the transition matrix  $\hat{K}$  in Eq. (2) in the wide-band approximation is given by the  $4 \times 4$  matrix:

$$\hat{K} = - \begin{pmatrix} 2f_-^{(1)} & -f_+^{(1)} & -f_+^{(1)} & 0 \\ -f_-^{(1)} & f_-^{(0)} + f_+^{(1)} & 0 & -f_+^{(0)} \\ -f_-^{(1)} & 0 & f_-^{(0)} + f_+^{(1)} & -f_+^{(0)} \\ 0 & -f_-^{(0)} & -f_-^{(0)} & 2f_+^{(0)} \end{pmatrix}, \quad (\text{S30})$$

where we have introduced

$$f_+^{(j)} := f_L^{(j)} + f_R^{(j)}, \quad f_-^{(j)} := 2 - f_+^{(j)}, \quad (\text{S31})$$

with the Fermi distribution

$$f_\alpha^{(j)}(\mu_\alpha(\theta), U(\theta)) := \frac{1}{1 + e^{\beta(\epsilon_0 + jU(\theta) - \mu_\alpha(\theta))}} \quad (\text{S32})$$

in the lead  $\alpha (= L \text{ or } R)$  for the single occupancy  $j = 0$  and double occupancy  $j = 1$ .

It is straightforward to obtain the eigenvalues of  $K(\Lambda(\theta))$  in Eq. (S30) as  $\varepsilon_0 = 0$ ,  $\varepsilon_1 = -f_+^{(0)} - f_-^{(1)}$ ,  $\varepsilon_2 = -4 - \varepsilon_1$ ,  $\varepsilon_3 = -4$ . The left and right eigenfunctions corresponding to  $\varepsilon_0 = 0$  of  $\hat{K}$  are given by

$$\langle \ell_0 | = (1, 1, 1, 1), \quad (\text{S33})$$

$$|r_0\rangle = \alpha_0 (f_+^{(0)} f_+^{(1)}, f_+^{(0)} f_-^{(1)}, f_+^{(0)} f_-^{(1)}, f_-^{(0)} f_-^{(1)})^T, \quad (\text{S34})$$

respectively, where  $\alpha_0 = [2(f_+^{(0)} + f_-^{(1)})]^{-1}$  is the normalization factor. As discussed in previous section, the eigen state corresponding to the zero eigenvalue denotes the nonequilibrium steady state, namely  $|r_0\rangle = |\hat{\rho}^{\text{SS}}\rangle$ . Note that  $|r_0\rangle$  satisfies  $\langle \ell_0 | r_0 \rangle = \text{Tr} \hat{\rho}^{\text{SS}} = 1$ . The left and right eigenfunctions corresponding to  $\varepsilon_1$ ,  $\varepsilon_2$ , and  $\varepsilon_3$  are, respectively, given by

$$\langle \ell_1 | = (f_-^{(1)}, \gamma, \gamma, -f_+^{(0)}), \quad (\text{S35})$$

$$|r_1\rangle = \alpha_1 (f_+^{(1)}, \gamma, \gamma, -f_-^{(0)})^T, \quad (\text{S36})$$

and

$$\langle \ell_2 | = (0, 1, -1, 0), \quad |r_2\rangle = \frac{1}{2}(0, 1, -1, 0), \quad (\text{S37})$$

and

$$\langle \ell_3 | = (f_-^{(0)} f_-^{(1)}, -f_-^{(0)} f_+^{(1)}, -f_-^{(0)} f_+^{(1)}, f_+^{(0)} f_+^{(1)}), \quad (\text{S38})$$

$$|r_3\rangle = \alpha_3 (1, -1, -1, 1)^T. \quad (\text{S39})$$

where  $\alpha_1 = 2[(f_+^{(0)} + f_-^{(1)})(f_+^{(1)} + f_-^{(0)})]^{-1}$ ,  $\alpha_3 = [2(f_-^{(0)} + f_+^{(1)})]^{-1}$ , and  $\gamma = (-f_+^{(0)} + f_-^{(1)})/2$ .

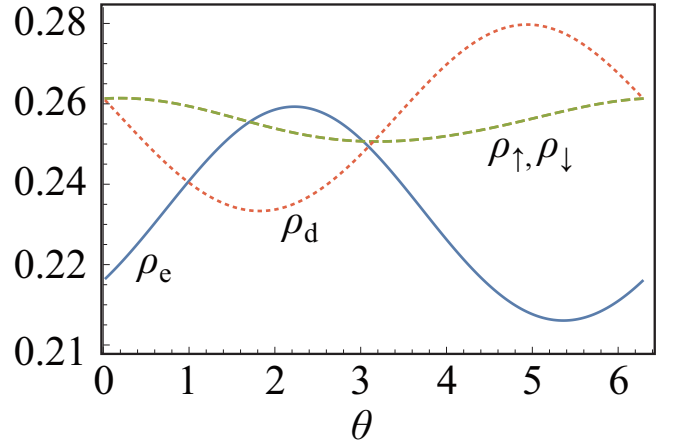


Figure S7. Time evolution of the elements of the density matrix.

### B. Time evolution of the density matrix for the Anderson model

We are interested in the entropy production in the first cycle  $\Delta S$  given by Eq. (5). For this purpose we need to know  $\hat{\rho}(2\pi)$  and  $\hat{\rho}(0)$ . The former is given by

$$\begin{aligned} |\hat{\rho}(2\pi)\rangle &= |\hat{\rho}^{\text{SS}}(2\pi)\rangle + \sum_{i=1}^3 C_i |r_i(2\pi)\rangle \\ &= \begin{pmatrix} \alpha_0 f_+^{(0)} f_+^{(1)} + C_1 \alpha_1 f_+^{(1)} + C_3 \alpha_3 f_-^{(0)} f_-^{(1)} \\ \alpha_0 f_+^{(0)} f_-^{(1)} + C_1 \alpha_1 \gamma - C_3 \alpha_3 f_-^{(0)} f_+^{(1)} \\ \alpha_0 f_+^{(0)} f_-^{(1)} + C_1 \alpha_1 \gamma - C_3 \alpha_3 f_-^{(0)} f_+^{(1)} \\ \alpha_0 f_-^{(0)} f_-^{(1)} - C_1 \alpha_1 f_-^{(0)} + C_3 \alpha_3 f_+^{(0)} f_+^{(1)} \end{pmatrix}, \end{aligned} \quad (\text{S40})$$

where  $\alpha_0 = [2(f_+^{(0)} + f_-^{(1)})]^{-1}$ ,  $\alpha_1 = 2[(f_+^{(0)} + f_-^{(1)})(f_+^{(1)} + f_-^{(0)})]^{-1}$ ,  $\alpha_3 = [2(f_-^{(0)} + f_+^{(1)})]^{-1}$ , and  $\gamma = (-f_+^{(0)} + f_-^{(1)})/2$ .

Figure S7 plots the time evolution of the elements of  $\hat{\rho}(\theta)$  as  $\rho_e$ ,  $\rho_d$ ,  $\rho_\uparrow$  and  $\rho_d$ . This figure clearly supports the positivity of all elements to keep the complete positivity.

### C. BSN connection for Anderson model

In this subsection, we present the explicit form of the BSN connection for the Anderson model. For the explicit calculation of the BSN connection, we use Eqs. (6) and (7) with  $\theta = 2\pi$ . Integrating by parts, one obtains

$$\begin{aligned} &\int_0^{2\pi} \langle \tilde{\ell}_2(\phi) | \frac{d}{d\phi} |r_0(\phi)\rangle \\ &= \int_0^{2\pi} e^{\epsilon^{-1} \int_\phi^{2\pi} \varepsilon_2(\xi) d\xi} \langle \ell_2(\phi) | \frac{d}{d\phi} |r_0(\phi)\rangle \\ &= \int_0^{2\pi} e^{\epsilon^{-1} \int_\phi^{2\pi} \varepsilon_2(\xi) d\xi} \left[ \frac{d}{d\phi} \langle \ell_2(\phi) | r_0(\phi) \rangle - \frac{d \langle \ell_2(\phi) |}{d\phi} |r_0(\phi)\rangle \right] \\ &= 0, \end{aligned} \quad (\text{S41})$$

where we have used that  $\langle \ell_2(\phi) \rangle$  is independent of  $\phi$ . Thus the summation of  $i$  in Eq. (6) reduces to the summation with  $i = 1$  and 3. The differentiation of  $|r_0(\phi)\rangle$  with respect to  $\phi$  becomes

$$\begin{aligned} & \frac{d}{d\phi} |r_0(\phi)\rangle \\ &= \left[ \frac{d}{d\phi} \frac{1}{2(f_+^{(0)} + f_-^{(1)})} \right] \begin{pmatrix} f_+^{(0)} f_+^{(1)} \\ f_+^{(0)} f_-^{(1)} \\ f_+^{(0)} f_-^{(1)} \\ f_-^{(0)} f_-^{(1)} \end{pmatrix} \\ &+ \frac{1}{2(f_+^{(0)} + f_-^{(1)})} \frac{d}{d\phi} \begin{pmatrix} f_+^{(0)} f_+^{(1)} \\ f_+^{(0)} f_-^{(1)} \\ f_+^{(0)} f_-^{(1)} \\ f_-^{(0)} f_-^{(1)} \end{pmatrix} \\ &= \alpha(\Lambda) |r_0\rangle + \frac{1}{2(f_+^{(0)} + f_-^{(1)})} \frac{d}{d\phi} \begin{pmatrix} f_+^{(0)} f_+^{(1)} \\ f_+^{(0)} f_-^{(1)} \\ f_+^{(0)} f_-^{(1)} \\ f_-^{(0)} f_-^{(1)} \end{pmatrix}, \quad (\text{S42}) \end{aligned}$$

where  $\alpha(\Lambda)$  is the unimportant factor because we are interested in  $\langle \ell_i(\phi) \frac{d}{d\phi} |r_0(\phi)\rangle$  with  $i \neq 0$  and  $\langle \ell_i(\phi) |r_0(\phi)\rangle = 0$  for  $i \neq 0$ .

Substitution of Eq. (S42) into Eq. (6) with  $\theta = 2\pi$  yields

$$|\hat{\rho}(2\pi)\rangle \simeq |r_0(2\pi)\rangle + \sum_{1,3} \mathcal{C}_i |r_i(2\pi)\rangle, \quad (\text{S43})$$

$$\mathcal{C}_i = - \int_0^{2\pi} d\phi \frac{\langle \tilde{\ell}_i(\phi) \rangle}{2(f_+^{(0)} + f_-^{(1)})} \frac{d}{d\phi} \begin{pmatrix} f_+^{(0)} f_+^{(1)} \\ f_+^{(0)} f_-^{(1)} \\ f_+^{(0)} f_-^{(1)} \\ f_-^{(0)} f_-^{(1)} \end{pmatrix}. \quad (\text{S44})$$

By using  $\frac{d}{d\theta} (f_+^{(j)} + f_-^{(j)}) = 0$ ,  $\mathcal{C}_i$  becomes

$$\begin{aligned} \mathcal{C}_i &= - \int_0^{2\pi} d\phi \frac{\langle \tilde{\ell}_i(\phi) \rangle}{2(f_+^{(0)} + f_-^{(1)})} \frac{df_+^{(0)}}{d\phi} \begin{pmatrix} f_+^{(1)} \\ f_-^{(1)} \\ f_-^{(1)} \\ -f_-^{(1)} \end{pmatrix} \\ &- \int_0^{2\pi} d\phi \frac{\langle \tilde{\ell}_i(\phi) \rangle}{2(f_+^{(0)} + f_-^{(1)})} \frac{df_+^{(1)}}{d\phi} \begin{pmatrix} f_+^{(0)} \\ -f_+^{(0)} \\ -f_+^{(0)} \\ -f_-^{(0)} \end{pmatrix}. \quad (\text{S45}) \end{aligned}$$

Substituting Eq. (S35) into Eq. (S45) we obtain

$$\begin{aligned} \mathcal{C}_1 &= - \int_0^{2\pi} d\phi e^{\epsilon^{-1} \int_\phi^{2\pi} \varepsilon_1(\xi) d\xi} \frac{2f_-^{(1)}}{f_+^{(0)} + f_-^{(1)}} \frac{df_+^{(0)}}{d\phi} \\ &- \int_0^{2\pi} d\phi e^{\epsilon^{-1} \int_\phi^{2\pi} \varepsilon_1(\xi) d\xi} \frac{2f_+^{(0)}}{f_+^{(0)} + f_-^{(1)}} \frac{df_+^{(1)}}{d\phi}. \quad (\text{S46}) \end{aligned}$$

Similarly, we obtain

$$\begin{aligned} \mathcal{C}_3 &= \int_0^{2\pi} d\phi e^{\epsilon^{-1} \int_\phi^{2\pi} \varepsilon_3(\xi) d\xi} \frac{f_+^{(1)} f_-^{(1)}}{f_+^{(0)} + f_-^{(1)}} \frac{df_+^{(0)}}{d\phi} \\ &- \int_0^{2\pi} d\phi e^{\epsilon^{-1} \int_\phi^{2\pi} \varepsilon_3(\xi) d\xi} \frac{f_+^{(0)} f_-^{(0)}}{f_+^{(0)} + f_-^{(1)}} \frac{df_+^{(1)}}{d\phi} \\ &= \int_0^{2\pi} d\phi e^{4\epsilon^{-1}(\phi-2\pi)} \frac{f_+^{(1)} f_-^{(1)}}{f_+^{(0)} + f_-^{(1)}} \frac{df_+^{(0)}}{d\phi} \\ &- \int_0^{2\pi} d\phi e^{4\epsilon^{-1}(\phi-2\pi)} \frac{f_+^{(0)} f_-^{(0)}}{f_+^{(0)} + f_-^{(1)}} \frac{df_+^{(1)}}{d\phi}. \quad (\text{S47}) \end{aligned}$$

As shown in Eq. (S47), the factor  $e^{4\epsilon^{-1}(\phi-2\pi)}$  in the integrand plays an important role. Thanks to this factor we do not need to consider the long time memory in the dynamics. In the case of  $\mathcal{C}_3$ , the scale factor does not depend on the choice of the trajectory but only depends on  $\theta$ . Thus, one can estimate the BSN curvature at  $\phi$ .

For  $\epsilon \ll 1$ , the exponential factor  $e^{4\epsilon^{-1}(\phi-2\pi)}$  behaves as the cut-off function and thus

$$\begin{aligned} \mathcal{C}_3 &\approx \int_{2\pi-\epsilon}^{2\pi} d\phi \left[ \frac{f_+^{(1)} f_-^{(1)}}{f_+^{(0)} + f_-^{(1)}} \frac{df_+^{(0)}}{d\phi} - \frac{f_+^{(0)} f_-^{(0)}}{f_+^{(0)} + f_-^{(1)}} \frac{df_+^{(1)}}{d\phi} \right] \\ &\sim \epsilon \left[ \frac{f_+^{(1)} f_-^{(1)}}{f_+^{(0)} + f_-^{(1)}} \frac{df_+^{(0)}}{d\phi} - \frac{f_+^{(0)} f_-^{(0)}}{f_+^{(0)} + f_-^{(1)}} \frac{df_+^{(1)}}{d\phi} \right]_{\phi=2\pi}. \quad (\text{S48}) \end{aligned}$$

Similarly, we can write

$$\mathcal{C}_1 \sim \epsilon \left[ \frac{2e^{\varepsilon_1(2\pi)}}{f_+^{(0)} + f_-^{(1)}} \left( f_-^{(1)} \frac{df_+^{(0)}}{d\phi} - f_+^{(0)} \frac{df_+^{(1)}}{d\phi} \right) \right]_{\phi=2\pi}. \quad (\text{S49})$$

From the above estimations, the leading order contribution of the geometrical phase is order  $O(\epsilon)$ .

Let us demonstrate that  $\mathcal{C}_i$  vanishes in the non-interacting case  $\beta U_0 = 0$ . In this case,  $f_\pm^{(0)} = f_\pm^{(1)} \equiv g_\pm$  and  $g_+ + g_- = 2$  and thus  $\mathcal{C}_i$  becomes

$$\begin{aligned} \lim_{\beta U_0 \rightarrow 0} \mathcal{C}_1 &= -2 \int_0^{2\pi} d\phi e^{\epsilon^{-1} \int_\phi^{2\pi} \varepsilon_1(\xi) d\xi} \frac{dg_+}{d\phi}, \\ \lim_{\beta U_0 \rightarrow 0} \mathcal{C}_3 &= 0. \quad (\text{S50}) \end{aligned}$$

Thus, the entropy production due to the geometrical term is absent in the case of  $U_0 = 0$ .

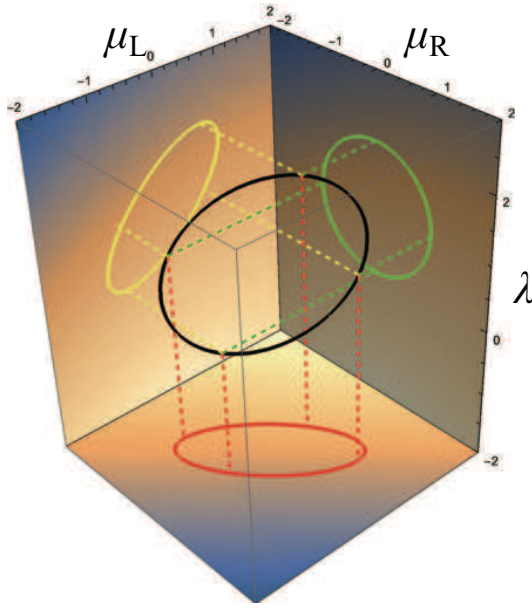


Figure S8. A schematic of control of parameters. We set  $r = 1$  and  $\delta = \pi/4$ .

In the opposite limit  $\beta U_0 \rightarrow \infty$ ,  $f_+^{(1)} = 0$ ,  $f_-^{(1)} = 2$  and  $C_i$  also vanishes since

$$\begin{aligned} \lim_{U_0 \rightarrow \infty} C_1 &= - \int_0^{2\pi} d\phi \frac{2}{f_+^{(0)}} \frac{df_+^{(0)}}{d\phi} \\ &= -2 \int_0^{2\pi} d\phi \frac{d \ln f_+^{(0)}}{d\phi} = 0, \\ \lim_{U_0 \rightarrow \infty} C_3 &= 0. \end{aligned} \quad (\text{S51})$$

Therefore, the entropy production due to the geometrical term is also absent in the limit  $\beta U_0 \rightarrow \infty$ .

#### D. Some detailed results for the Anderson model

In this section, we present some detailed results beyond the main text as well as a figure of control parameters in the parameter space.

First, let us plot the control parameters in parameter space. Figure S8 is a schematic of the control parameters in parameter space.

Now, let us present some detailed results of the calculation of the Anderson model beyond the main text. In Fig. S9, we plot  $C_1$  (left figure),  $C_3$  (right figure) against  $\delta$  for various  $r$  with fixed  $\beta U_0 = 0.1$ . As shown the coefficients increases as  $r$  increases. The coefficients  $C_1$  and  $C_3$  become zero at  $\delta = \pi$ .

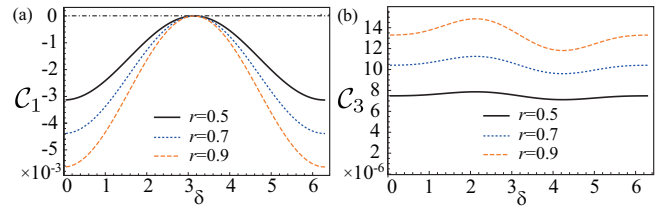


Figure S9. Plots of  $C_1$  (left figure) and  $C_3$  (right figure) against  $\delta$  for  $r = 0.5, 0.7, 0.9$  where  $\beta U_0 = 0.1$ .

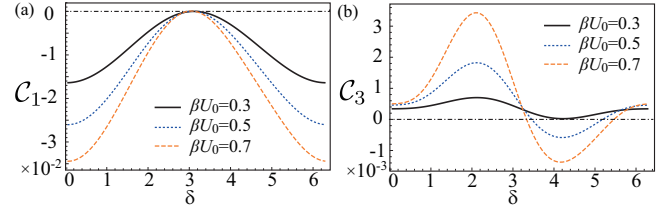


Figure S10. Plots of  $C_1$  (left figure) and  $C_3$  (right figure) against  $\delta$  for  $\beta U_0 = 0.3, 0.5, 0.7$  with  $r = 0.9$ .

Figure S10 shows that coefficients  $C_1$  (left figure),  $C_3$  (right figure) for various  $\beta U_0$  with fixed  $r = 0.9$ . As shown in Fig. S10  $|C_i$  with  $i = 1$  and  $3$  increases with  $\beta U_0$ .

We plot the one-cycle averaged relative entropy  $\overline{S^{\text{HS}}}(\theta) := \frac{1}{2\pi} \int_{\theta}^{\theta+2\pi} d\phi S^{\text{HS}}(\hat{\rho}(\phi) || \hat{\rho}^{\text{SS}}(\phi))$  in Fig. S11 for  $\delta = 0$ ,  $r = 0.9$ , and  $\beta U_0 = 0.1$ . This figure also indicates the oscillation of  $\overline{S^{\text{HS}}}(\hat{\rho}(\theta) || \hat{\rho}^{\text{SS}}(\theta))$  which increase at some instance.

#### IV. DIFFERENCE BETWEEN REF. [S32] AND THE PRESENT STUDY

If we assume that  $|\hat{\rho}(\theta)\rangle$  depends on  $\theta$  only through modulation parameters  $\mathbf{\Lambda}$  as in Ref. [S32], we can express  $|\hat{\rho}^{(1)}(\mathbf{\Lambda}(\theta))\rangle := (\hat{\rho}(\theta) - \hat{\rho}^{\text{SS}}(\theta))/\epsilon$  as

$$|\hat{\rho}^{(1)}(\mathbf{\Lambda}(\theta))\rangle = \hat{K}^+(\mathbf{\Lambda}(\theta)) \frac{d}{d\theta} |\hat{\rho}^{\text{SS}}(\mathbf{\Lambda}(\theta))\rangle \quad (\text{S52})$$

which is used in Ref. [S32].

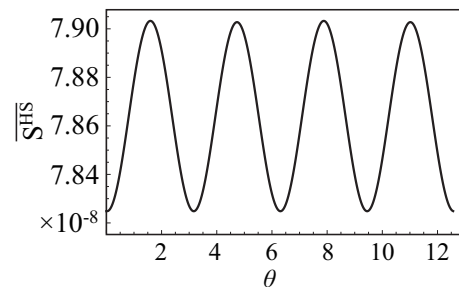


Figure S11. Sequential plots of time averaged relative entropy  $\overline{S^{\text{HS}}}(\theta)$  for  $\delta = 0$ ,  $r = 0.9$  and  $\beta U_0 = 0.1$ .

If  $|\hat{\rho}(\theta)\rangle$  explicitly depends on  $\theta$ , Eq. (S52) cannot be used. To clarify the difference, let us consider the relaxation process in the absence of the parameter modulation, in which the time evolution of the density matrix is given by

$$\begin{aligned} |\hat{\rho}(\theta)\rangle &= |\hat{\rho}^{\text{SS}}\rangle + \sum_{i \neq 0} e^{\int_0^\theta d\theta \frac{\varepsilon_i}{\epsilon}} |r_i\rangle \\ &= |\hat{\rho}^{\text{SS}}\rangle + \sum_{i \neq 0} e^{\frac{\varepsilon_i}{\epsilon} \theta} |r_i\rangle \\ &= |\hat{\rho}^{\text{SS}}\rangle + \sum_{i \neq 0} e^{-\frac{|\varepsilon_i|}{\epsilon} \theta} |r_i\rangle. \end{aligned} \quad (\text{S53})$$

The density matrix relaxes to the steady state  $|\hat{\rho}^{\text{SS}}\rangle$  in the long time limit  $\theta/\epsilon \gg 0$ . We note that this limit is usually achieved not by  $\theta \gg 1$  but by  $\epsilon \rightarrow 0$ . It is obvious that  $\epsilon \rightarrow 0$  is the singular limit and the expansion via  $\epsilon$  is not available since the convergence radius of  $e^{-1/x}$  is zero. Thus, if the density matrix explicitly depends on  $\theta$ , we may not use the expansion via  $\epsilon$  as in Ref. [S32].

- 
- [S1] H. Hayakawa, V. M. M. Paasonen, and R. Yoshii, “Geometrical Quantum Chemical Engine”, arXiv:2112.12370 (2021).  
[S2] T. Sagawa and H. Hayakawa, Geometrical expression of excess entropy production, Phys. Rev. E **84**, 051110 (2011).

- [S3] T. Yuge, T. Sagawa, A. Sugiura, and H. Hayakawa, Geometrical Excess Entropy Production in Nonequilibrium Quantum Systems, J. Stat. Phys. **153**, 412 (2013).  
[S4] R. Yoshii and H. Hayakawa, “Analytical expression of geometrical pumping for a quantum dot based on quantum master equation”, arXiv:1312.3772